Modeling and simulation of the industrial production of aluminium: the nonlinear approach*

J.-F. Gerbeau[†], T. Lelièvre, and C. Le Bris[‡]

December 16, 2002

Abstract

We report on the numerical simulation of the industrial production of aluminium. The motion of the two non miscible conducting fluids is modeled through the incompressible Navier-Stokes equations coupled with the (parabolic) Maxwell equations. Stabilized finite elements techniques and an Arbitrary Lagrangian Eulerian formulation (for the motion of the interface separating the two fuids) are used in the numerical simulation. The industrial problem and the modeling strategy are presented in details. An outline of the numerical analysis of the problem, with a special emphasis on conservation and stability properties is provided. Examples of numerical simulations of the industrial case are eventually presented.

Keywords: industrial problem; aluminium production; magnetohydrodynamic; free interface; two-fluids flow; surface tension; geometric conservation law; ALE formulation.

---

*This article has been presented by the third author (CLB) as a plenary lecture at the AMIF conference, April 2002, Lisbon.

[†]INRIA, Rocquencourt B.P.105, 78153 LE CHESNAY Cedex, France, jean-frederic.gerbeau@inria.fr

[‡]CERMICS,Ecole Nationale des Ponts et Chaussées, 6 & 8 Av. Pascal, 77455 Champs-sur-Marne, France, {lelievre,lebris}@cermics.enpc.fr

Contents

1 Introduction

We report here on a long-term work on the modeling and the numerical simulation of an electrolysis cell used for the industrial production of aluminium. We shall first present the challenging issues raised by this problem. Next, we isolate some modelling difficulties, which are of general interest. We show how we solved or circumvented them. In one sentence, our approach can be summarized as follows: we conduct a deep mathematical analysis of the models, then we focus on the nonlinearities on the problem, and simulate their consequences on the behaviour of the system, thereby complementing linear approaches that are more commonly developed in the literature.

For the sake of brevity, we shall not go here into the details neither on the mathematical analysis of the models, nor on the numerical analysis of the methods. We shall only give an outline of the techniques we have adopted or developed, and present significant simulations we have performed. For more details, we refer the interested reader to other publications of us: [7, 11, 12, 13, 14, 15, 16, 17, 18, 19, 20, 21, 22]. In particular, a companion article [21] presents a thorough account of the numerical analysis.

1.1 The industrial problem

The industrial production of aluminium is a problem of outstanding difficulty. The aluminium is produced from an aluminium oxyde $\mathrm{Al_2O_3}$, itself coming from a native form, bauxite. In presence of Carbon, the aluminium oxyde $\mathrm{Al_2O_3}$ is reduced into pure aluminium. Thermodynamically, the reduction can only occur around 1000 degrees Celsius, a temperature at which Aluminium is a liquid. Let us briefly indicate that a schematic picture of the functioning of the electrolysis cell is as follows (*see* [27]) : an electric current of the order of 10^5 A runs through two horizontal layers of conducting incompressible fluids, namely a bath of the aluminium oxyde above, and a layer of liquid aluminium below, which is the aluminium produced "so far" (*see* Figure 1). The oxydoreduction reaction takes place both at the interface between the two fluids

$$Al_2O_3 + 6\,e^- \longrightarrow 2\,Al^{3+} + 3\,O^{2-} + 6\,e^- \longrightarrow 2\,Al + 3\,O^{2-} \tag{1}$$

and at the surface of anods, which provide the bath with the Carbon needed for the reaction:

$$3\,O^{2-} + 3/2\,C \longrightarrow 3/2\,C0_2(\text{gas}) + 6\,e^- \,. \tag{2}$$

The global balance reads

$$2\,Al_2\,O_3 + 3\,C \longrightarrow 4\,Al + 3\,CO_2 \tag{3}$$

The difference of electric potential needed for the oxydoreduction is small (around a few Volts) but the intensity of the current is so large that the electric power spent in the cell is huge. The reason why the intensity of the electric current is taken so large is of course that the quantity of aluminium produced in the cell is proportional to the intensity (accordingly to (1)). For an intensity such as 10^5 A, the production is typically of a few tons of aluminium per cell and per day. A plant of production of aluminium consists in one (or many) line(s) of, say, 250 cells connected in series. The electric power needed for the whole plant is typically of the order of magnitude of that produced by one unit of a contemporary nuclear plant.

With a view to reducing the power waste, the distance between the carbon anods covering the top of the cell and the surface of the aluminium layer (a perfectly conducting fluid directly connected to the cathode at the bottom of the cell) is to be kept as small as possible. Indeed, as the intensity needs to be kept as large as possible, diminishing the power amounts to diminishing the difference of potential. The latter, which is bounded from below by the potential needed for the oxydoreduction to occur, is also due to the potential drop in the (badly conducting) upper fluid of the cell. The goal is therefore to keep the thickness of the upper fluid layer as small as possible. This thickness is called the *anod-metal distance* which is a self explanatory term. Typically, the order of magnitude of the anod-metal distance is of a few centimeters vertically, which is a very tiny distance with respect to the horizontal sizes of the cell which are of the order of many meters, say 4 by 10 to fix the ideas. In addition to this penalizing aspect ratio, the main difficulty in trying to diminish the anod-metal distance lies in the fact that, due to the presence of the electric current, the conducting fluids experience strong Lorentz forces (the induced magnetic field is of the order of 0.01 T) and therefore move (the typical flow velocity in the cell is 0.2 m/s). This causes movement of the interface, which separates the two fluids. This movement may lead to instabilities. The anod-metal ditance should be small to reduce the cost ; however, this distance should be sufficiently large to avoid short-circuits: this optimization is an experimental challenge. Let us indeed emphasize that if the interface between the two fluids ever touches the anod, the consequences may be dramatic, as is easily understandable when a short-circuit occurs at such huge powers. There is even the possibility of destroying the series of cells. The challenge is all the more difficult as the intensity used in the cell becomes larger and larger, which is indeed the case with the endless seek for financial profit. As is often the case for industrial processes, the maximum pay-off that is dreamed of will be obtained by adopting risky strategies, on the borderline of instabilities.

1.2 A need for numerical simulations

The stage is now set. It is understandable that controlling and optimizing such an industrial process is not an easy task. An electrolysis cell is kind of a wicked environment, where precise experimental observations are difficult to make. Even monitoring the phenomena at play inside the cell is a challenge: high temperature, corrosive medium,.... Controlling and optimizing is one step further. In such a framework, numerical simulation can efficiently complement the experimental strategy, and advantageously compensate for its weaknesses.

We intend to address in further research the optimal control problem, say:

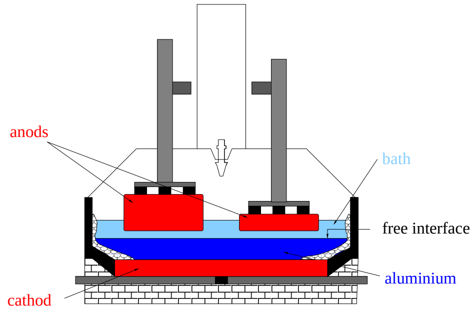

Figure 1: An aluminium cell: vertical cut.

how to stabilize the position of the interface? Which parameter should be used ? is it possible in practice ? In such industrial problems, it should indeed be born in mind that the practical constraints are of enormous impact: some actual control parameters are the height of anods, the intensity, the shape of the conducting wires bringing the current to and from the cell. These parameters cannot be tuned in real time. This is a feature that must be accounted for, one way or another, when posing the optimization problem.

But for the time being, as a preliminary and necessary step before attacking the optimization problem, and also as a step which has its own interest, we have concentrated our efforts on the direct simulation problem. It was expected that the results of careful numerical simulations could give a valuable insight into the understanding of the phenomena inside the cell, and therefore implicitly help to optimize it. It is indeed the case. But before we describe the modeling strategy we have employed, two comments are in order.

First, the fact that experimental observations are difficult, and therefore rather incomplete, to the least, has another consequence than that of giving full value to the strategy of numerical simulation. It also precisely renders this strategy difficult, because of the lack of complete reliable measurements. As only a few measures are available, the question is indeed how to obtain definite conclusions about the validity of the numerical simulations. In order to overcome, as far as possible, this difficulty, we have chosen both (a) to validate our algorithms on academic test problems, and (b) to try and recover in "real" simulations phenomena well known in the engineering world, or recipes well known by engineers of the field. This has proven to be a reasonable strategy in such a context, so far.

Second, it is useful to mention at this point the possible numerical approaches for this problem. Simplifying assumptions have to be done, due to the overwhelming number of physical phenomena involved in the functioning of the cell, namely (i) magnetohydrodynamics (MHD), (ii) moving interface, (iii) ferromagnetism (the material the boundaries are made of is ferromagnetic), (iv) electrochemistry (the concentration of the chemical species is not homogeneous throughout the bath, which has some impact on the global behaviour of the cell), (v) three-phase flows (bubbles of carbon oxydes at the surface of anods (see (2)), solidification process at the boundaries), (vi) temperature effects (which influences the value of the physical parameters, in particular). Usually, a continuum, purely fluid, description is chosen. Items (iv), (v) and (vi) are neglected, or postponed to specifically dedicated studies, item (iii) is accounted for in establishing the boundary condition for the magnetic field. Apart from the present work, the existing approaches are essentially based upon the use of mechanical/physical arguments to guess recipes for stability, possibly together with a strategy of numerical simulation based upon a linearization procedure applied to the equations at the vicinity of the equilibrium state, followed by a linear stability analysis. Instances of such works are [4, 5, 6, 32, 33, 36, 38].

2 The modeling strategy

Our strategy has been to adopt a genuine nonlinear approach, where no linearization at all is made (at the continuous level). As taught to us by analysis on test situations (even in radically different contexts), a nonlinear stability analysis, as the one needed here to study the stability of the interface between the two fluids, can only come out from direct numerical simulations. This has been our bottom line. Of course, we only have succeeded in our program at the price of doing other simplifying assumptions, none of them related to nonlinearity issues.

Therefore, we start with the very complete system consisting of the Maxwell equations coupled to the multifluid Navier-Stokes equations, and then try to reduce the complexity by carefully imposing simplifying assumptions we have total control upon. The system we start from therefore reads

$$\partial_t \rho + \operatorname{div}(\rho \mathbf{u}) = 0, \tag{4}$$

$$\left\{ \begin{aligned} \partial_t(\rho\mathbf{u}) + \operatorname{div}(\rho\mathbf{u}\otimes\mathbf{u}) - \operatorname{div}(2\eta\epsilon(\mathbf{u})) + \nabla p &= \rho\mathbf{f} + \frac{1}{\mu}\,\mathbf{curl}\,\mathbf{B}\times\mathbf{B} \\ \operatorname{div}\mathbf{u} &= 0 \end{aligned} \right. \tag{5}$$

$$\left\{ \begin{aligned} \partial_t\mathbf{B} + \mathbf{curl}\,\mathbf{E} &= 0 \\ \operatorname{div}\mathbf{B} &= 0 \\ -\partial_t(\varepsilon\mathbf{E}) + \mathbf{curl}\,\frac{\mathbf{B}}{\mu} &= \mathbf{j} \end{aligned} \right. \tag{6}$$

$$\mathbf{j} = \sigma(\mathbf{E} + \mathbf{u}\times\mathbf{B}), \tag{7}$$

where one recognizes (from (4) to (7)) the mass conservation equation, the incompressible two-fluids Navier-Stokes equations, the Maxwell equations and Ohm's law. We introduce ρ to denote the density of the fluids (it is a piecewise constant function), $\mathbf{u}$ the velocity field, $\mathbf{B}$ the magnetic field, $\mathbf{E}$ the electric field, $\mathbf{j}$ the current, $\mathbf{f}$ the body force (gravity), p the pressure field, and $\boldsymbol{\epsilon}(\mathbf{u})$ the deformation gradient $(\nabla\mathbf{u} + \nabla\mathbf{u}^T)/2$. The electrical conductivity σ and the viscosity η are assumed to be known functions of ρ.

It turns out that, as such, system (4)-(5)-(6)-(7) cannot be studied mathematically, due to the hyperbolic nature of the Maxwell equations, and is not tractable numerically either. As a matter of fact, this system is likely to be not necessary for the situation at hand. We indeed believe, that a simpler system, both well-posed mathematically and tractable numerically, suffices to correctly reproduce the behaviour of the cell. It is obtained from the full system (4)-(5)-(6)-(7) by neglecting the $\partial_t(\varepsilon \mathbf{E})$ term (low frequency hypothesis), and, less important, by setting $\mu = \mu_0$. This allows one to eliminate the unknown $\mathbf{E}$, and to obtain a system with the only unknowns $\mathbf{u}$, p, ρ, $\mathbf{B}$.

The governing equations we shall use are thus the time-dependent incompressible Navier-Stokes equations for two viscous immiscible fluids (4)-(5) coupled with the Maxwell equations in their parabolic form (*see* [26] for example):

$$\begin{aligned} \partial_t \mathbf{B} + \mathbf{curl}\,(\frac{1}{\mu_0 \sigma}\mathbf{curl}\,\mathbf{B}) &= \mathbf{curl}\,(\mathbf{u} \times \mathbf{B}), && (8)\\ \operatorname{div} \mathbf{B} &= 0. && (9) \end{aligned}$$

These equations are set on a fixed bounded domain Ω of $\mathbb{R}^d$ (with $d = 2$ or 3), and complemented with the magnetic boundary conditions

$$(\mathbf{B} \cdot \mathbf{n})|_{\partial\Omega} = \text{given}, \qquad (\mathbf{curl}\,\mathbf{B} \times \mathbf{n})|_{\partial\Omega} = \text{given}, \tag{10}$$

and for the hydrodynamic boundary conditions, pure slip on the side walls and no-slip elsewhere. The initial conditions read: $\rho|_{t=0} = \rho^0$, $\mathbf{u}|_{t=0} = \mathbf{u}^0$ and $\mathbf{B}|_{t=0} = \mathbf{B}^0$, where $\mathbf{u}^0$ and $\mathbf{B}^0$ are divergence free vector fields. The density of each fluid is assumed to be constant at $t = 0$, a property which is propagated in time by (4), the volume of each fluid being then preserved.

Let us emphasize again that no additional simplification will be made on these equations and that we shall therefore deal with all the nonlinearities of this strongly coupled system of PDEs. The mathematical analysis of this system, as well as the foundation of it on the basis of a whole hierarchy of possible models, is an issue that has already been dealt with in a series of previous works: existence of solution to (4)-(5)-(8)-(9) in [13], regularity of the flow and of the interface in [7], long-time behaviour of the hydrodynamics two fluid system in [15], regularity of the Navier-Stokes equation in [17].

In particular, it is to be emphasized that the system we shall employ cannot be simplified further naively, for instance by considering that the electromagnetic phenomena are so more rapid than the hydrodynamic ones that they can be considered as stationary (which is indeed a tempting assumption). It would lead (even in the one-fluid case, see the details in [14, 18]) to an ill-posed mathematical system consisting of a coupling between the time dependent Navier Stokes equations and the stationary Maxwell equations, i.e. the static form of (8). Consequently, if one wants to use the stationary Maxwell equation, then one needs also to consider the stationary Navier-Stokes equations, i.e. the static version of (4)-(5). From the theoretical viewpoint, studying mathematically this purely static system requires to answer the open mathematical question: can one prove existence of a solution to the steady-state two-fluids Navier-Stokes equations? In spite of the fact that the existence of solution is an open question (see however [28]), we shall nevertheless try in our computations to reach the infinite time limit of (4)-(5)-(6)-(7) and thus the steady state version of our time dependent equations. It indeed is of primary interest to determine the steady state in practice. Let us emphasize the crucial message : the choice of system (4)-(5)-(8)-(9) is supported by a rigorous mathematical analysis (in the limit of course of the capabilities of the current mathematical techniques, see [13]).

From the numerical viewpoint, the simulation of system (4)-(5)-(8)-(9) requires to understand the following issues

- how to conveniently discretize the MHD coupling,
- what type of finite elements should be used,
- how to deal with the motion of the interface, and to ensure, when necessary, the motion of the mesh,
- how to ensure the conservation of the mass of each fluid and the energy stability in the time dependent simulation.

Let us briefly say here that we use an Arbitray Lagrangian Eulerian formulation to move the interface and the mesh, that we take care of having a discrete energy inequality and a conservation of mass using a discretization scheme that ensures a geometric conservation law. Apart from the above issues, we have also examined (in [21]) the numerical strategy to properly account for the surface tension term when such a term is added to the right-hand side of (4), either for physical reasons or as a numerical artefact. For the sake of brevity, we however leave this question aside here.

We concentrate in the remainder of this article on the numerical strategies we used to answer to the above questions, together with a rapid exposition of the results we obtained.

For computational purposes, it proves convenient after a rewriting of the preceeding equations in non-dimensional form (for which we refer to [21]), to eliminate the body force in one fluid, in the spirit of the method described in [19]. This trick greatly improves the robustness of the numerical computations. As far as the non-dimensional numbers are concerned, let us only mention that they are seven of them: the Reynolds numbers $Re_i = \dfrac{\rho_i U L}{\eta_i}$ (of the order of 10^5 in our application), the magnetic Reynolds numbers $Rm_i = \mu_0 \sigma_i L U$ (10^{-1} in one fluid, 10^{-5} in the other one), the coupling parameter $S = \dfrac{B^2}{\mu_0 \rho_1 U^2}$ (of the order of 1), the Froude number $F = \dfrac{U^2}{gL}$, the density ratio $M = \dfrac{\rho_2}{\rho_1}$. The simulations we shall present in Section 4 make use of non-dimensional numbers that are one or two orders of magnitude smaller than in reality. In particular, the Reynolds number will be taken 100 times as small as the real one, which can be interpreted as a somewhat vague way to account for turbulence effects.

It is a concern of us to perform computations with the physically relevant non-dimensional numbers within a near future.

To begin with, we concentrate, in Subsection 3.1, on the difficulties in the numerical simulation of the coupled MHD problem in the case of one single fluid, postponing the specific difficulties due to the presence of two fluids to Subsection 3.2. The numerical computations of (4)-(5)-(8)-(9) we show in Section 4 are obtained by a combination of all the techniques of Section 3.

3 Numerical strategies

3.1 The one-fluid MHD equations

With a view to focusing on the MHD coupling, we come back as announced to the one-fluid case, and therefore consider the system

$$\begin{cases} \rho\partial_t \mathbf{u} + \rho\mathbf{u}\cdot\nabla\mathbf{u} - \operatorname{div}(2\eta\epsilon(\mathbf{u})) + \nabla p &= \rho\mathbf{f} + \dfrac{1}{\mu_0}\mathbf{curl}\,\mathbf{B}\times\mathbf{B} \\ \operatorname{div}\mathbf{u} &= 0 \\ \partial_t\mathbf{B} + \mathbf{curl}\,(\dfrac{1}{\mu_0\sigma}\mathbf{curl}\,\mathbf{B}) &= \mathbf{curl}\,(\mathbf{u}\times\mathbf{B}) \\ \operatorname{div}\mathbf{B} &= 0 \end{cases}$$

where ρ is a constant throughout the domain. The system is supplied with *ad hoc* boundary and initial conditions. It is straightforward to show that, due to a cancellation of terms in the right-hand side, the solution satisfies the energy equality

$$\frac{1}{2}\frac{d}{dt}\int_\Omega\left(\rho|\mathbf{u}|^2 + \frac{|\mathbf{B}|^2}{\mu_0}\right) + \int_\Omega\left(\frac{1}{\sigma}\frac{|\mathbf{curl}\,\mathbf{B}|^2}{\mu_0^2} + \eta|\nabla\mathbf{u}|^2\right) = \int_\Omega \rho\mathbf{f}\cdot\mathbf{u} \qquad (11)$$

The fact that this estimate of energy is to be reproduced at the discrete level will be a guide for our discretization strategy. For the sake of simplicity, let us detail how we iterate inside the coupling terms in the case of the stationary version of the above equations, written in non-dimensional form:

$$\begin{cases} -\dfrac{1}{Re}\triangle\,\mathbf{u} + \mathbf{u}\cdot\nabla\mathbf{u} + \nabla p &= S\,\mathbf{curl}\,\mathbf{B}\times\mathbf{B} + \frac{1}{F}\mathbf{f} \\ \dfrac{1}{Rm}\mathbf{curl}\,(\mathbf{curl}\,\mathbf{B}) &= \mathbf{curl}\,(\mathbf{u}\times\mathbf{B}) \end{cases}$$

Basically, one can at first think of a segregated algorithm of the following type

$$\begin{aligned} -\frac{1}{Re}\triangle\,\mathbf{u}^{n+1} + \mathbf{u}^n.\nabla\mathbf{u}^{n+1} + \nabla p^{n+1} &= S\,\mathbf{curl}\,\mathbf{B}^n\times\mathbf{B}^n + \tfrac{1}{F}\mathbf{f} \\ \frac{1}{Rm}\mathbf{curl}\,(\mathbf{curl}\,\mathbf{B}^{n+1}) &= \mathbf{curl}\,(\mathbf{u}^{n+1}\times\mathbf{B}^{n+1}) \end{aligned} \qquad (12)$$

It may be proven that the above algorithm needs a good amount of damping, and is only conditionally stable. On the other hand, a more efficient strategy is to design a fully coupled algorithm in the following way

$$\left\{\begin{array}{rcl}\mathbf{u}^n\cdot\nabla\mathbf{u}^{n+1}-\dfrac{1}{Re}\triangle\,\mathbf{u}^{n+1}+\nabla p^{n+1}+S\,\mathbf{B}^n\times\mathbf{curl}\,\mathbf{B}^{n+1} & = & \frac{1}{F}\mathbf{f}\\ \dfrac{1}{Rm}\mathbf{curl}\,(\mathbf{curl}\,\mathbf{B}^{n+1})-\mathbf{curl}\,(\mathbf{u}^{n+1}\times\mathbf{B}^n) & = & 0,\end{array}\right. \tag{13}$$

(Both systems (12) and (13) are complemented by the divergence free constraints $\mathrm{div}\,\mathbf{u}^{n+1}=0$, $\mathrm{div}\,\mathbf{B}^{n+1}=0$), where it should be noted that the special discretization of the coupling terms allows one to recover an energy estimate of the form (11) at the discrete level. In addition, the above algorithm is unconditionally stable (provided that the continuous solution is unique).

When implementing algorithm (13) in a finite element type method, a specific feature appears, that we now wish to underline. Even if the magnetic equation (second line of (13)) is diffusion dominated, it is actually necessary to use a stabilization technique for it. A stabilization method for the fully coupled MHD equation has thus been developed (see [12]).

Let us also briefly mention that various methods for solving the magnetic equation (second line of (13)) have been tested in [11, 16]. We also refer to the latter work for the description of some numerical methods to impose the boundary conditions (10).

The consideration of classical benchmarks of the MHD literature such as the Hartmann flow ("magnetic version" of the hydrodynamic Poiseuille flow) has allowed us to validate the above numerical strategy, see [21]. Incidentally, let us mention that such numerical experiments also indicate that turbulence effects are very specific in a MHD framework which convinced us to deliberately forget them, in the absence of any deep understanding of turbulence for such MHD flows.

In addition, a simple one-fluid model for the real electrolysis cell has been designed and the influence of the shape of the wires and the distribution of the external current upon the behaviour of the hydrodynamic flow inside the cell has been investigated. Again, this has been found to be in good qualitative agreement with well known behaviours.

3.2 The two-fluids MHD equations

We now come back to the two-fluid MHD problem. With respect to the previous section, the extension is now to simulate the motion of the free interface between the two fluids. As no topological change of the interface is expected (it is reasonable to assume that it remains the graph of a function), and as a great accuracy is needed in the determination of its position (as the anod-metal distance is the central issue that heavily influences the behaviour of the cell, as explained above), we have chosen to explicitly track the interface and therefore have adapted an Arbitrary Lagrangian Eulerian formulation to the present context of a MHD flow. The ALE formulation for *one* fluid with a free surface has been used by several authors, for example [39, 40, 31, 25, 1, 3, 24]. In the case of two fluids, see for example [35], and in the framework of MHD, see [2].

As for the computation of the domain velocity field $\mathbf{w}$, we have chosen a special form for it, namely $\mathbf{w}^n = (0, 0, w)$, at each time step t_n, and define it as the solution of

$$\left\{\begin{array}{rcll} -\triangle w & = & 0 & \text{on } \Omega_i^n, i = 1, 2, \\ w & = & \dfrac{\mathbf{u}^n \cdot \mathbf{n}}{n_z} & \text{on } \Sigma^n, \\ \dfrac{\partial w}{\partial n} & = & 0 & \text{on } \partial\Omega. \end{array}\right. \tag{14}$$

This special determination allows us to ensure the following Geometric Conservation Law (in the spirit of [23, 30, 34] in the framework of the finite volume method, [10] in the framework of finite element methods, and [29] for fluid structure interaction problems):

$$\begin{aligned} \int_{\Omega_i^{n+1}} \psi(x)\, dx - \int_{\Omega_i^n} \psi \circ \mathcal{A}_{n,n+1}(y)\, dy &= \delta t \int_{\Omega_i^n} \psi \circ \mathcal{A}_{n,n+1}(y) \mathrm{div}_y \mathbf{w}^n\, dy \\ &= \delta t \int_{\Omega_i^{n+1}} \psi(x) \mathrm{div}_x \mathbf{w}^n \circ \mathcal{A}_{n,n+1}^{-1}(x)\, dx \end{aligned} \tag{15}$$

for any ψ defined on Ω_i^{n+1}, where $\mathcal{A}_{n,n+1}$ is the discretization in time of the function that maps the reference domain onto the current one.

Relation (15) is the discrete analogue of the continuous formula

$$\frac{d}{dt} \int_{\Omega(t)} \psi(x,t)\, dx = \int_{\Omega(t)} \frac{\partial \psi}{\partial t}\Big|_{\hat{x}}\, dx + \int_{\Omega(t)} \psi(x,t)\, \mathrm{div}\, \mathbf{w}\, dx.$$

This being done, we are in position to ensure two key properties for our global algorithm: first, the conservation of the mass of each fluid, and second, the stability in the energy norm. Both of these properties are easy to fulfill on a fixed mesh, but have seemed to us not so trivial to ensure in the ALE setting. The above GCL is one ingredient to ensure both these properties. More explicitely, when (i) the normal vectors at the nodes of the free interface $\Sigma(t)$ are computed so as to have (see also [8]) $\displaystyle\int_\Sigma \mathbf{u}_h \cdot \mathbf{n}_h\, d\sigma = \int_{\Omega_1} \mathrm{div}\, \mathbf{u}_h\, dx$, (ii) the condition $\displaystyle\int_{\Omega_1} \mathrm{div}\, \mathbf{u}_h\, dx = 0$ holds, and (iii) GCL is satisfied, then we can first prove that the mass of each fluid is conserved at the discrete level. Second, denoting by $\displaystyle E^n = \int_{\Omega^n} \frac{\rho |\mathbf{u}^n|^2}{2}\, dy + \int_{\Omega^n} \frac{|\mathbf{B}^n|^2}{2\mu_0}\, dy$ the total energy of the system, we may show, again because of the above three properties (i)-(ii)-(iii), that the discrete analogue of (11) holds (for convenient simple data), namely (see [21])

$$\frac{E^{n+1} - E^n}{\delta t} + \int_{\Omega^{n+1}} 2\eta |\boldsymbol{\epsilon}(\mathbf{u}^{n+1})|^2\, dx + \int_{\Omega^{n+1}} \frac{1}{\mu_0 \sigma} |\mathbf{curl}\, \mathbf{B}^{n+1}|^2\, dx \leq 0.$$

As was the case for the issues examined in the previous subsection, we also have tested the above numerical methodology on classical benchmarks. In addition, we have checked that the properties (i)-(ii)-(iii) are in some sense optimal in order to obtain the conservation of the mass of each fluid. For instance, test cases have shown that when the displacement field for the mesh $\mathbf{w}$ is assumed to be the solution of

$$\left\{ \begin{array}{rcll} -\triangle\, \mathbf{w} & = & 0 & \text{on } \Omega_i^n, i = 1, 2, \\ \mathbf{w} & = & \mathbf{u} & \text{on } \Sigma^n, \\ \dfrac{\partial \mathbf{w}}{\partial n} & = & 0 & \text{on } \partial\Omega, \end{array} \right. \tag{16}$$

instead of (14), so that the GCL property does not hold anymore, then the mesh is distorsed as time evolves, and a modification of the mass is indeed observed, thus condition (iii) is "necessary". Likewise, we have shown through test cases, that condition (ii) is also instrumental: it can be ensured using discontinuous finite elements for the discretization of the pressure (for example with the mixed elements Q2/P1), or using continuous finite elements while imposing with a Lagrange multiplier that the numerical flux $\displaystyle\int_{\Sigma^n} \mathbf{u}_h^n \cdot \mathbf{n}_h \, d\sigma$ through the interface vanishes (see [9]). Then, the conservation of mass holds. It has been experimentally checked that it does not hold otherwise in the context of continuous finite elements for the pressure.

4 Numerical simulations

4.1 The steady state of the cell

We have performed computations on realistic cells, however on a simplified geometry (but a real aspect ratio), with a viscosity two orders of magnitude as large as the real one (for both transient and steady-state calculations) and boundary conditions on the magnetic field divided by 10 (for transient calculations). The boundary conditions on the magnetic fields are taken either from experimental measures or from independent numerical simulations of the magnetic field created by the conductors around the cell. The aim of our simulations is to recover some well known phenomenological parameters (e.g. the number of vortices : *see* [12]) and to have an insight into some parameters that are difficult to measure (e.g. the shape of the interface between the bath and the metal).

In this article, we present in Figure 2 the result of a computation on a cell with a simplified (nevertheless relevant) circuit of conductors. The electric current in the cell is 90 kA and the dimensions of the cell are about $3 \times 9 \times 1.5$ m. For Biot and Savart computations (giving the boundary conditions on the magnetic field), we use either linear or parallelepipedic conductors. This interface has been obtained by computing the solution of the time-dependent system after a long time. On Figure 3, we show the result of a steady state calculation for a typical cell (the position of the interface is assumed to be known from a previous computation). The four swirls shown are effectively observed in reality and the magnitude of the velocities is rather close to the experimentally measured one.

Despite the fact we have artificially decreased the Reynolds number (for transient and steady-state calculations) and the magnetic field on the boundary (transient calculations), our results turn out to be in good qualitative agreement (shape of the interface, number of swirls) and even quantitative agreement (magnitudes of velocity in the steady-state calculation) with the experimental observations.

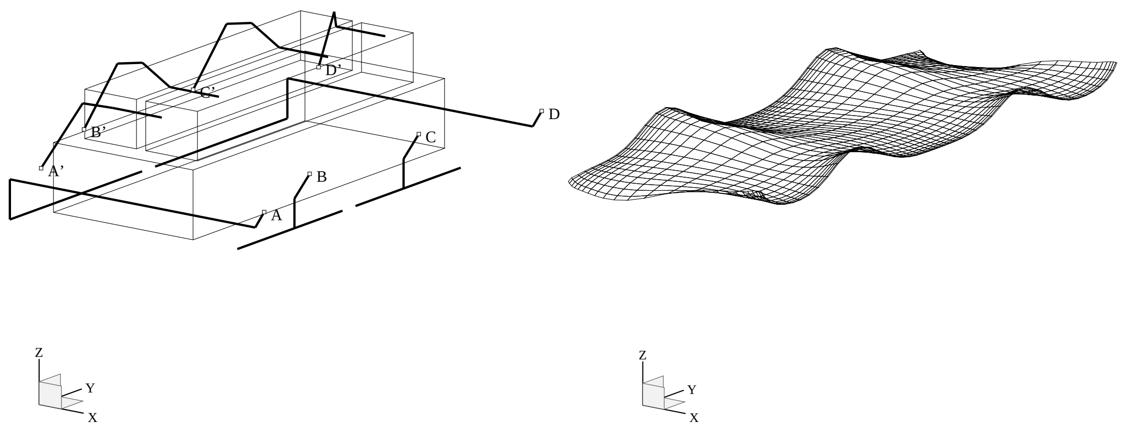

Figure 2: On the right, the shape of the interface at large time. The circuit of conductors is represented on the left.

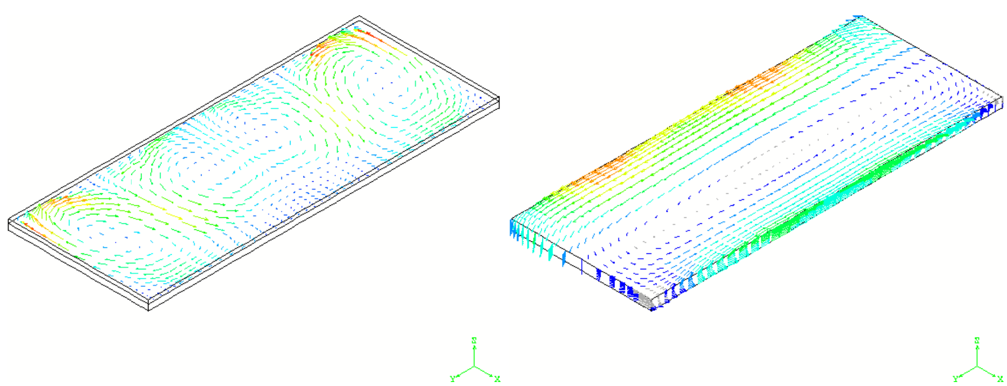

Figure 3: Left: velocity profile in the cell in a plane situated 5 cm under the interface. Velocity is between 1 cm.s^{-1} and 9 cm.s^{-1}. Right: magnetic field on the boundary of the cell.

4.2 The rolling phenomenon

One of the phenomena which is observed in industrial cells and which has been thoroughly investigated with a view to understanding it, forecasting it and avoiding it, is *metal pad rolling*. It is an oscillation of the cryolite / aluminium interface with a period ranging from five seconds up to more than one minute (see [27]). The physical origin of the phenomenon is a "constructive" interaction between the vertical component B_z of the magnetic field and a possible horizontal perturbed electric current, which results in a possibly instable rotating motion of the interface. It has been reported on that the metal can even get out of the cell in some cases ! Most studies, in the vein of [37, 4], are based upon a linearization procedure that leads to a definite criterion on the stability or unstability of a given cell, depending on its geometry, parameters,... In [4], the authors assert that a cylindrical cell becomes instable whatever the vertical field B_z. With a view to test this strong result of instability, we have developped a numerical simulation (see [20, 21]) that has shown that actually the situation is not truly described by the linearized system. For large B_z, our time dependent simulations show an interface that is indeed unstable, in accordance to the conclusions of the linearized study. But, there exists some B_z, small enough and not ridiculously small, for which the same time dependent simulation shows a stable motion of the interface. Of course, one could argue that, for times larger than those reached in our numerical simulations, the motion of the interface indeed becomes unstable, as predicted by the linearization study. But we wish then to make the following point. From a practical viewpoint, the goal is to understand what happens when the nominal functioning of the cell is unfortunately perturbed by an exterior event (say a change of anod in the cell, or in the cell nearby, or ...), which generally happens over a definite time window. Thus the perturbation is turned off after a while. This is exactly the conditions we have imposed for our time dependent simulation. The pertinent issue is then to know whether this "bounded in time" perturbation will durabily unstabilize the interface, or if the instability will vanish after a while. Typically, this type of transient external conditions are out of reach of the linearization studies, which are more binary, in some sense, but also more predictive in the infinite time limit. This explains why there is room for both approaches.

Of course, definite conclusions about this comparison between the two approaches are yet to be obtained, but this test case demonstrates the capability of our nonlinear approach to simulate complex MHD phenomena. In the past, these phenomena were analyzed with models based on many simplifications of the original equations providing excellent qualitative results, most of the time. But the influences of such simplifications need in any case to be tested and may become not negligible when precise results are desired. We have demonstrated that we can reproduce qualitatively the results predicted by simplified models, but that we are also able to give *quantitative* informations on the transient evolution of the system. This capability should have practical implications in the study of the instabilities of industrial cells.

Acknowledgements. We gratefully acknowledge the support from Aluminium Pechiney, LRF. At Pechiney, we wish to thank more particularly J. Colin de Verdière, J.M. Gaillard, N. Ligonesche, together with P. Homsi and C. Vanvoren for interesting and stimulating interactions over the years. We benefited from the constant help and advice of M. Bercovier (Hebrew University, Jerusalem) and P.L. Lions (Université Paris Dauphine). JP. Boujot is warmly thanked for initiating the project in the early 1990s.

References

[1] T.A. Baer, R.A. Cairncross, P.R. Schunk, P.A. Sackinger, and R.R. Rao. A finite element method for free surface flows of incompressible fluids in three dimensions. Part II: dynamic wetting line. *Int. Jour. Num. Meth. Fluids*, 33:405–427, 2000.

[2] J.U. Brackbill and W.E. Pracht. An implicit, almost lagrangian algorithm for magnetohydrodynamics *J. Comput. Phys.*, 13:455–482, 1973.

[3] R.A. Cairncross, P.R. Schunk, T.A. Baer, R. Rao, and P.A. Sackinger. A finite element method for free surface flows of incompressible fluids in three dimensions. Part I: Boundary fitted mesh motion. *Int. Jour. Num. Meth. Fluids*, 33:375–403, 2000.

[4] P.A Davidson and R.I. Lindsay. Stability of interfacial waves in aluminium reduction cells. *J. Fluid Mech.*, 362:273–295, 1998.

[5] J. Descloux, M. Flueck, and M.V. Romerio. Modelling for instabilities in hall-heroult cells : mathematical and numerical aspects. *Magnetohydrodynamics in Process Metallurgy*, pages 107–110, 1991.

[6] J. Descloux, M. Flueck, and M.V. Romerio. Stability in aluminium reduction cells : a spectral problem solved by an iterative procedure. *Light Metal*, pages 275–281, 1994.

[7] B. Desjardins and C. Le Bris. Remarks on a nonhomogeneous model of Magnetohydrodynamics, Differential and Integral Equations, 11, 3, pages 377-394, 1998.

[8] M.S. Engelman, R.L. Sani and P.M. Gresho. The implementation of normal and/or tangential velocity boundary conditions in finite element codes for incompressible fluid flow. *Int. J. Num. Meth. Fluids*, 2(3):225–238, 1982.

[9] L. Formaggia, J.-F. Gerbeau, F. Nobile, and A. Quarteroni. Numerical treatment of defective boundary conditions for the navier-stokes equations. *SIAM Journal on Numerical Analysis*, 40(1):376–401, 2002.

[10] L. Formaggia and F. Nobile. A stability analysis for the arbitrary Lagrangian Eulerian formulation with finite elements. *East-West J. Numer. Math.*, 7(2):105–131, 1999.

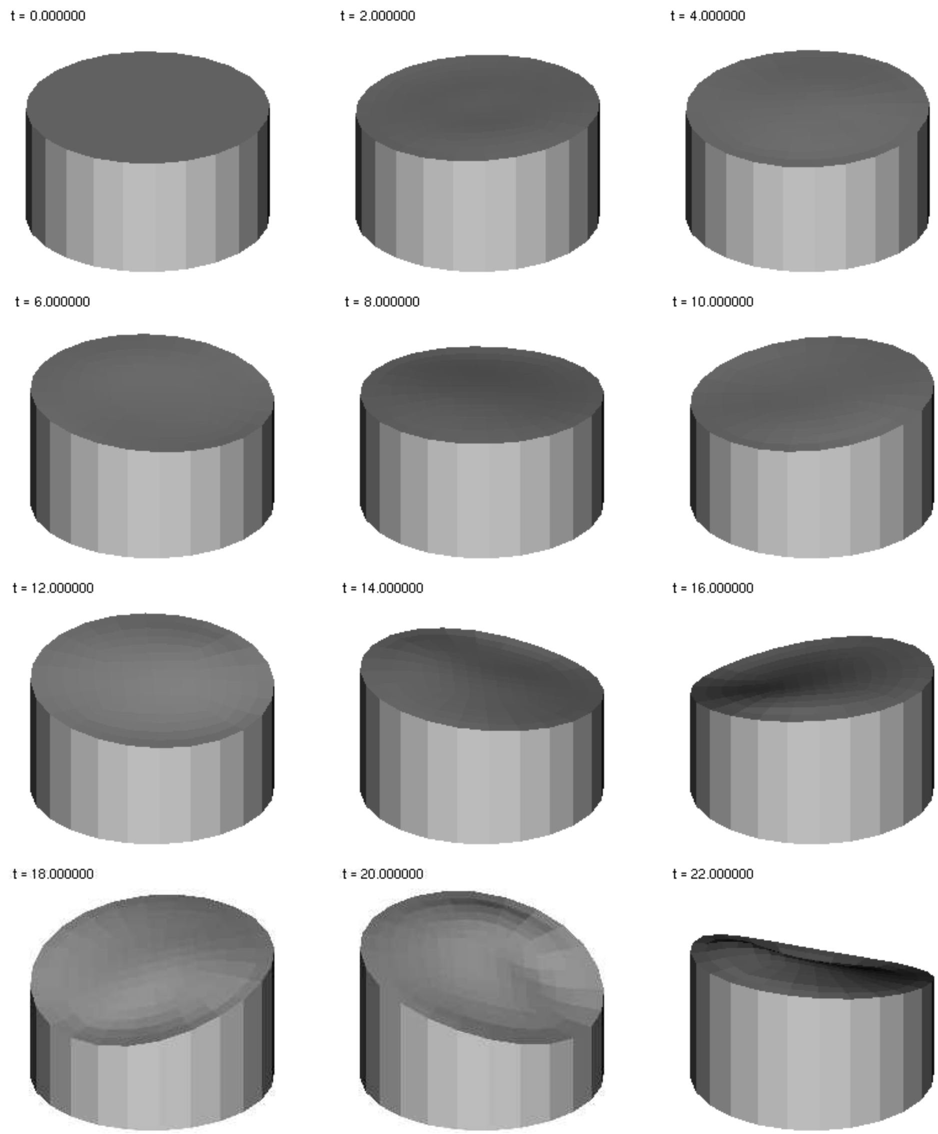

Figure 4: The phenomenon of metal pad rolling in a circular cell. Visualization of the interface and the lower fluid (the upper fluid is not represented for the sake of clarity). This is a case with B_z large. Reprinted from [21], with permission from Elsevier Science.

[11] J.-F. Gerbeau. Comparison of numerical methods for solving a magnetostatic problem. Application to the magnetohydrodynamic equations. In *Proceedings of the Fourth European Computational Fluid Dynamics, ECCOMAS 98*, pages 821–825. Wiley, 1998.

[12] J.-F. Gerbeau. A stabilized finite element method for the incompressible magnetohydrodynamic equations. *Numerische Mathematik*, 87(1):83–111, 2000.

[13] J.-F. Gerbeau and C. Le Bris. Existence of solution for a density-dependent magnetohydrodynamic equation. *Advances in Differential Equations*, 2(3):427–452, May 1997.

[14] J.-F. Gerbeau and C. Le Bris. On a coupled system arising in magnetohydrodynamics. *Appl. Math. Lett.*, 12:53–57, 1999.

[15] J.-F. Gerbeau and C. Le Bris. On the long time behaviour of the solution to the two-fluids incompressible navier-stokes equations. *Differential Integral Equations*, 12(5):691–740, 1999.

[16] J.-F. Gerbeau and C. Le Bris. Comparison between two numerical methods for a magnetostatic problem. *Calcolo*, 37(1):1–20, 2000.

[17] J.-F. Gerbeau and C. Le Bris. A basic remark on some Navier-Stokes equations with body forces. Applied Mathematics Letters, 13, pp 107-112, 2000.

[18] J.-F. Gerbeau and C. Le Bris. Mathematical study of a coupled system arising in Magnetohydrodynamics 6th International Conference on evolution equations and their applications in physical and life sciences, Eds. Lumer & Weis, pp 355-367, 2000, Marcel Dekker.

[19] J.-F. Gerbeau, C. Le Bris, and M. Bercovier. Spurious velocities in the steady flow of an incompressible fluid subjected to external forces. *Int. Jour. Num. Meth. Fluids*, 25:679–695, October 1997.

[20] J.-F. Gerbeau, T. Lelièvre, C. Le Bris, and N. Ligonesche. Metal pad roll instabilities. Proceedings of 2002 TMS (The Minerals, Metals & Materials Society), Seattle, February 2002.

[21] J.-F. Gerbeau, T. Lelièvre, and C. Le Bris. Simulations of MHD flows with moving interfaces. to appear in *J. Comp. Phys.*

[22] J-F. Gerbeau, T. Lelièvre, and C. Le Bris. Numerical simulations of two-fluids MHD flows. *Fundamental and Applied MHD. Proceedings of the Fifth international Pamir Conference*, p. I.101-I.105, 2002.

[23] H. Guillard and C. Farhat. On the significance of the geometric conservation law for flow computations on moving meshes. *Comput. Methods Appl. Mech. Engrg.*, 190(11-12):1467–1482, 2000.

[24] L.W. Ho. *A Legendre spectral element method for simulation of incompressible unsteady viscous free-surface flows.* PhD thesis, Massachussets Institute of Technology, 1989.

[25] A. Huerta and W. K. Liu. Viscous flow with large surface motion. *Comp. Meth. Appl. Mech. Engng.*, 69:277–324, 1988.

[26] W.F. Hughes and F.J. Young. *The electromagnetodynamics of fluids.* Wiley, 1966.

[27] A.F. LaCamera, D.P. Ziegler, and R.L. Kozarek. Magnetohydrodynamics in the Hall-Héroult process, an overview. *Light Metals*, pages 1179–1186, 1992.

[28] C. Le Bris, P.L. Lions and N. Masmoudi. *Work in preparation.*

[29] P. Le Tallec and J. Mouro. Fluid structure interaction with large structural displacements. *Comput. Meth. Appl. Mech. Engrg.*, 190:3039–3067, 2001.

[30] M. Lesoinne and C. Farhat. Geometric conservation laws for flow problems with moving boundaries and deformable meshes and their impact on aeroelastic computations. *Computer Methods in Applied Mechanics and Engineering*, 134:71–90, 1996.

[31] B. Maury. Characteristics ALE methods for the unsteady 3D Navier-Stokes equations with a free surface. *Comp. Fluid. Dyn.*, 6:175–188, 1996.

[32] R. Moreau and J.W. Evans. An analysis of the hydrodynamics of aluminium in reduction cells. *J. Electrochem. Soc.: Electrochem. Sci. Tech.*, 131(10):2251–2259, 1984.

[33] R. Moreau and D. Ziegler. The moreau-evans hydrodynamic model applied to actual hall-hroult cells. *Metal. Trans. B.*, 19B:737–744, 1988.

[34] B. Nkonga and H. Guillard. Godunov type method on nonstructured meshes for three-dimensional moving boundary problems. *Comput. Methods Appl. Mech. Engrg.*, 113(1-2):183–204, 1994.

[35] H.K. Rasmussen, O. Hassager, and A. Saasen. Viscous flow with large fluid-fluid interface displacement. *Int. Jour. Num. Meth. Fluids*, 28:859–881, 1998.

[36] M. Segatz and C. Droste. Analysis of magnetohydrodynamic instabilities in aluminium reduction cells. *Light Metals*, pages 313–322, 1994.

[37] T. Sele. Instabilities of the metal surface in electrolytic cells. *Light Metal*, pages 7–24, 1977.

[38] A.D. Sneyd and A. Wang. Interfacial instability due to mhd mode coupling in aluminium reduction cells. *J. Fluid Mech.*, 263:343–359, 1994.

[39] A. Soulaïmani, M. Fortin, G. Dhatt, and Y. Ouellet. Finite element simulation of two- and three dimensional free surface flows. *Comp. Meth. Appl. Mech. Engng*, 86:265–296, 1991.

[40] A. Soulaïmani and Y. Saad. An arbitrary Lagrangian-Eulerian finite element method for solving three-dimensional free surface flows. *Comput. Meth Appl. Mech Engrg.*, 162:79–106, 1998.